Progress Report

Ayse Irmak, Ph.D. Assistant Professor

School of Natural Resources, Department of Civil Engineering, and Center for Advanced Land Management Information Technology (CALMIT)

University of Nebraska-Lincoln, 311 Hardin Hall, Lincoln, NE 68583, U.S.A.
E-mail: airmak2@unl.edu; Phone: (402) 472-8024

TABLE OF CONTENTS **PAGE**

Project objectives

The overall goal of this project is to use the METRIC algorithms to produce area-specific ET maps that can be used to characterize and describe the dynamics of ET with Landsat and MODIS data. The specific objectives are to develop, test and demonstrate the tools that will take these ET maps and turn them into immediately usable products for planning, managing and regulating groundwater resources. The Nebraska Department of Natural Resources, Natural Resources Districts and the University of Nebraska will work together to develop, test and demonstrate tools that will take these ET maps and turn them into usable products for planning, managing and regulating groundwater resources. The tools/products to be developed and demonstrated include:

(1) Developing daily and seasonal ET maps for areas irrigated by groundwater sources and surface water across Republican and Platte river basins as well as other parts of NE.

(2) Sampling of project area to refine locally calibrated Kc curves for specific crops [i.e. corn, soybeans, alfalfa, sorgum, wheat,] and

(3) Developing a hydrological data assimilation scheme using regional ET data from METRIC data for better predictions of hydrological states, in particularly, ET and soil moisture, at a regional scale with Land Surface Model (LSM)/Land Information System (LIS) model.

Progress to date

METRIC was run with the inputs (weather, soil properties, water balance, etc.) for individual Landsat Path and Row (Fig. 1). Individual ET maps for 2007 have been generated from Landsat 5 and Landsat 7 satellite imagery with METRIC.

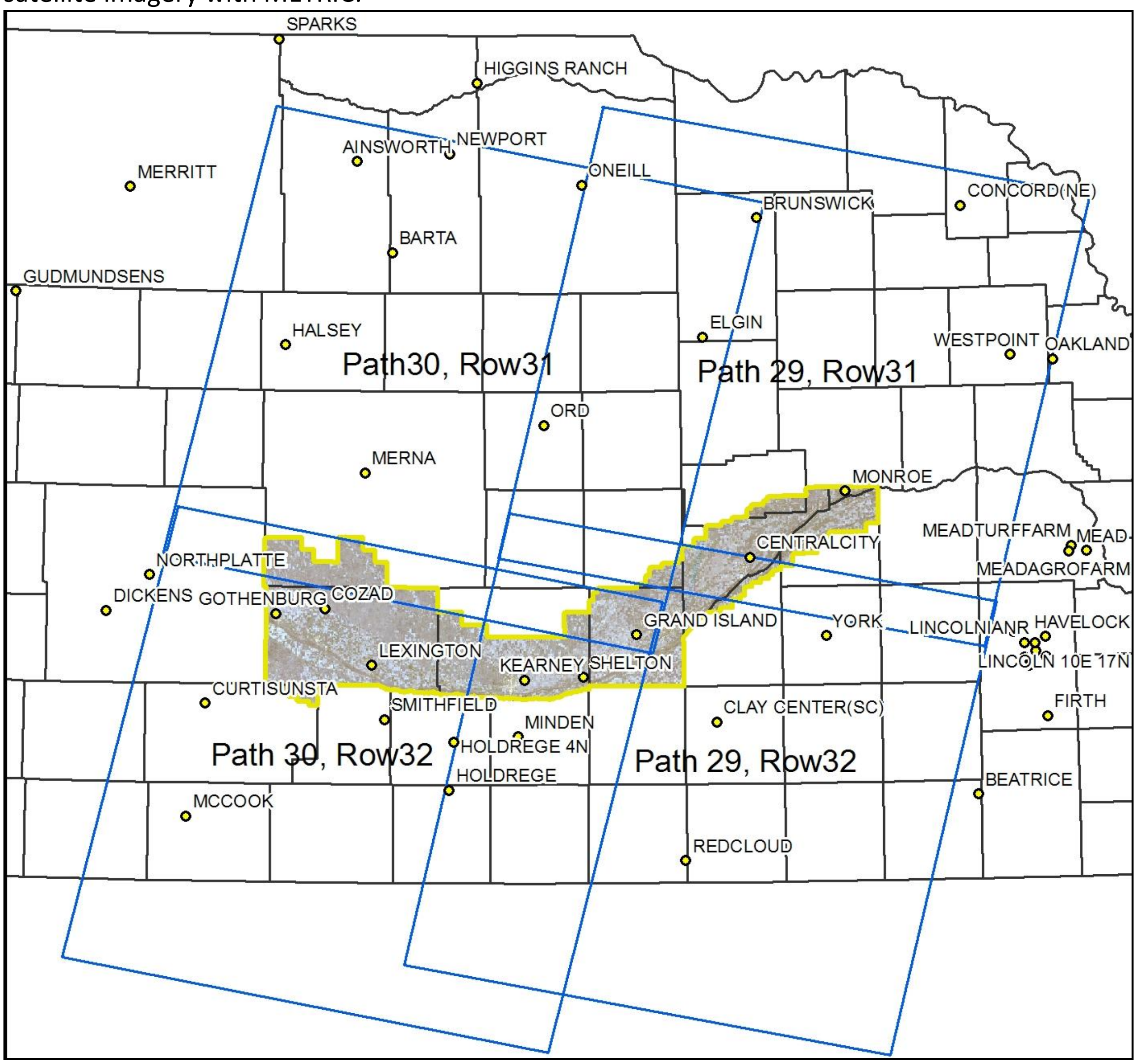

Figure 1. Study area showing weather station locations (yellow circles) and Landsat image footprints (blue lines).

Meteorological Data

Weather data were acquired from the High Plains Regional Climate Center's (HPRCC) Automated Weather Data Network (AWDN). The AWDN stations record hourly data for air temperature, humidity, soil temperature, wind speed and direction, solar radiation, and precipitation. Reference ET (ET_r) values were calculated using the ASCE-EWRI (2005) standardized Penman-Monteith equation for alfalfa reference generated from the Ref-ET software developed by the University of Idaho. Hourly precipitation and ET_r values were summed together to compute daily, 24-hour, ET_r values. Instantaneous and daily ET_r values were used for calibration of METRIC model.

Data from the Central City, Grand Island, Merna, and Smithfield stations were used for the generation of intermediate and final METRIC products from the individual images. It should be noted that other surrounding stations will used to create an interpolated (Spline or Kriging) map of reference ET for the project area to be used with the monthly and seasonal ET maps.

The Central City station was used in processing Landsat images for path 29 row 31, the Grand Island station was used for path 29 row 32, the Merna station was used for path 30 row 31, and the Smithfield station was used for path 30 row 32. The characteristics of four AWDN stations used in the project are given in Table 1.

Table 1. AWDN stations coordinates and characteristics.

Station	Path	Row	Latitude	Longitude	Elevation (m)
Central City	29	31	41.15	97.97	517
Grand Island	29	32	40.88	98.5	507
Merna	30	31	41.45	99.77	809
Smithfield	30	32	40.58	99.67	768

The weather data was quality controlled rigorously following the recommendations of Allen (1996) and ASCE-EWRI (2005). For example, observed solar radiation values were compared with calculated clear sky solar radiation (Figure 2-6). Of the four stations used for ET calculations, only Central City was considered in need of minor correction (Figure 3). Corrections are only applied when the data exhibits systematic errors. Individual values are not corrected for. Reasons for errors in the solar radiation values can be due to misalignment or miscalibration of the sensor. The Central City solar radiation data was corrected by increasing the values by 5% for days after 29 April 2007. Figure 4 shows observed solar radiation and clear sky solar radiation values after correction was applied.

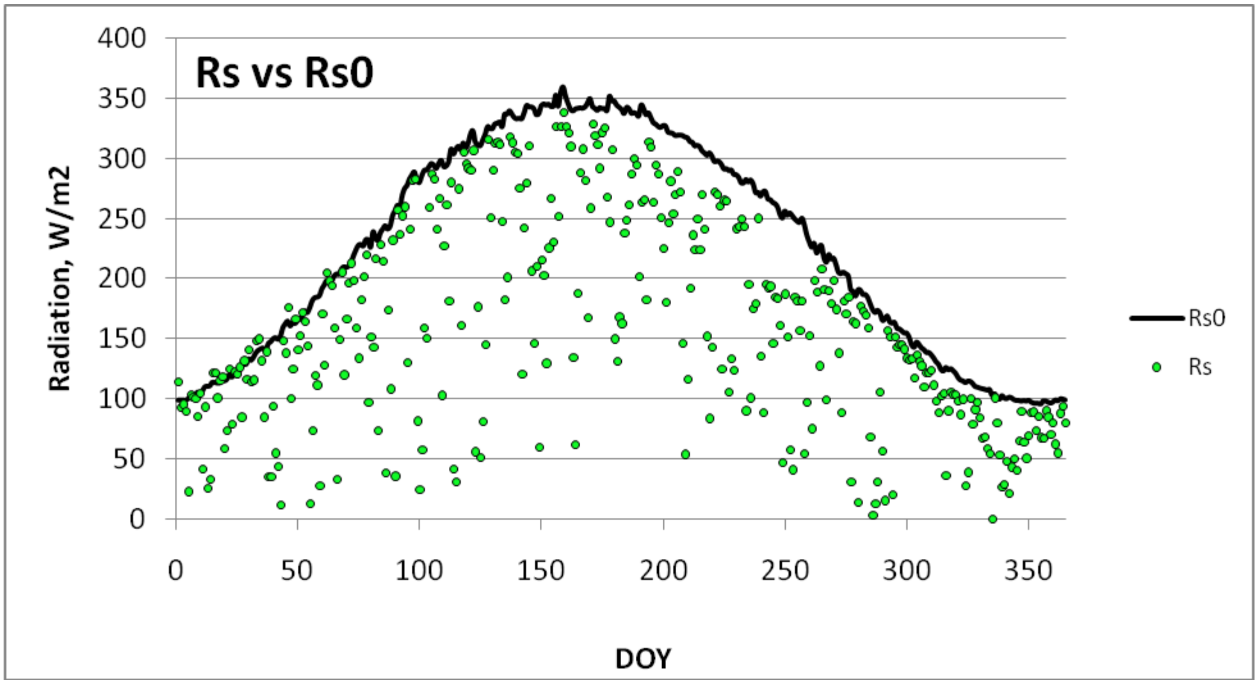

Figure 2. Original observed solar radiation (Rs, W/m^2) and calculated clear sky solar radiation (Rso, W/m^2) for 2007 from the Central City HPRCC AWDN weather station.

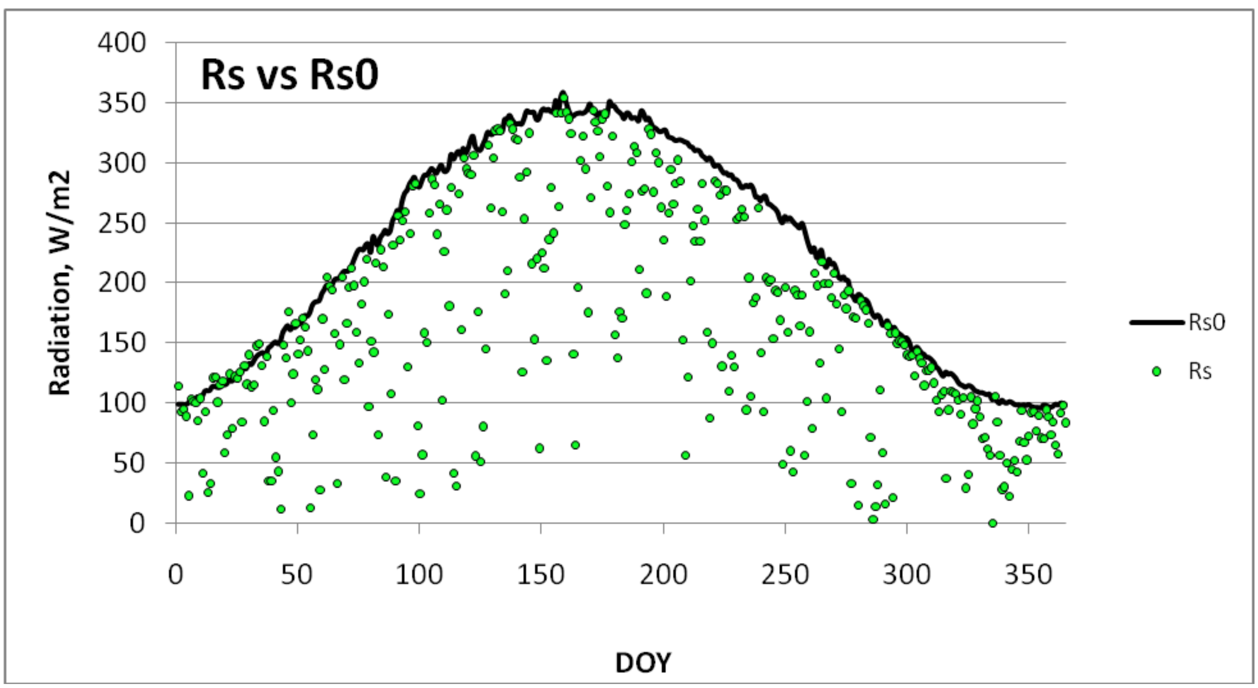

Figure 3. Corrected observed solar radiation (Rs, W/m^2) and calculated clear sky solar radiation (Rso, W/m^2) for 2007 from the Central City HPRCC AWDN weather station. Observed solar radiation (W/m^2) values were increased by 5% after 29 April 2007.

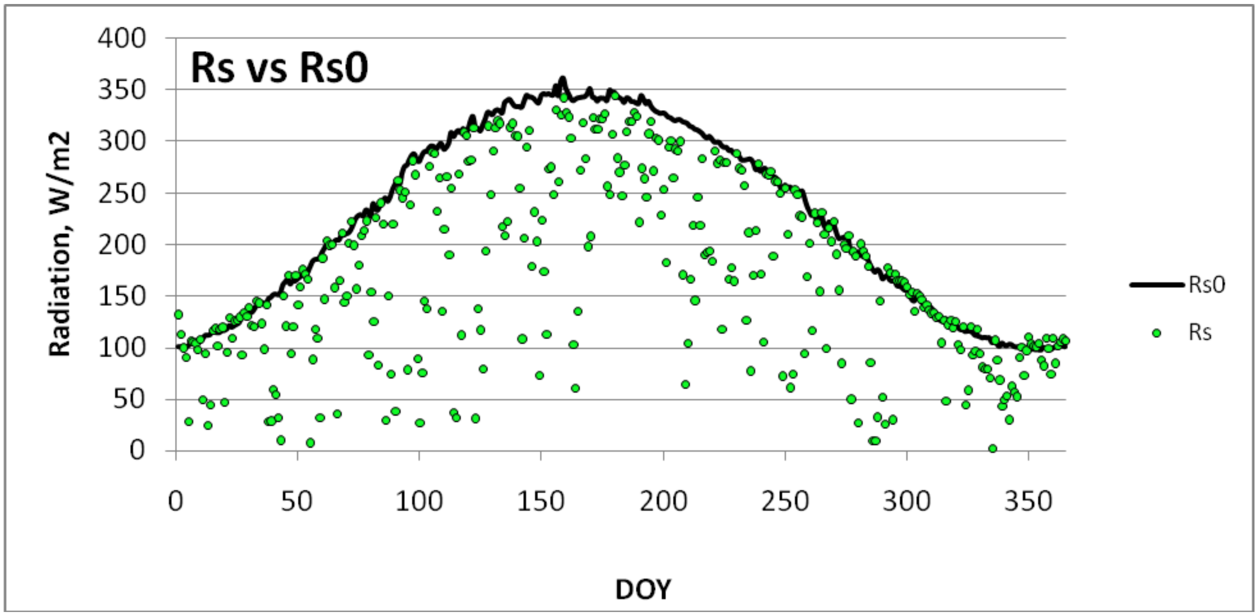

Figure 4. Observed solar radiation (W/m^2) and calculated clear sky solar radiation (W/m^2) for 2007 from the Grand Island HPRCC AWDN weather station.

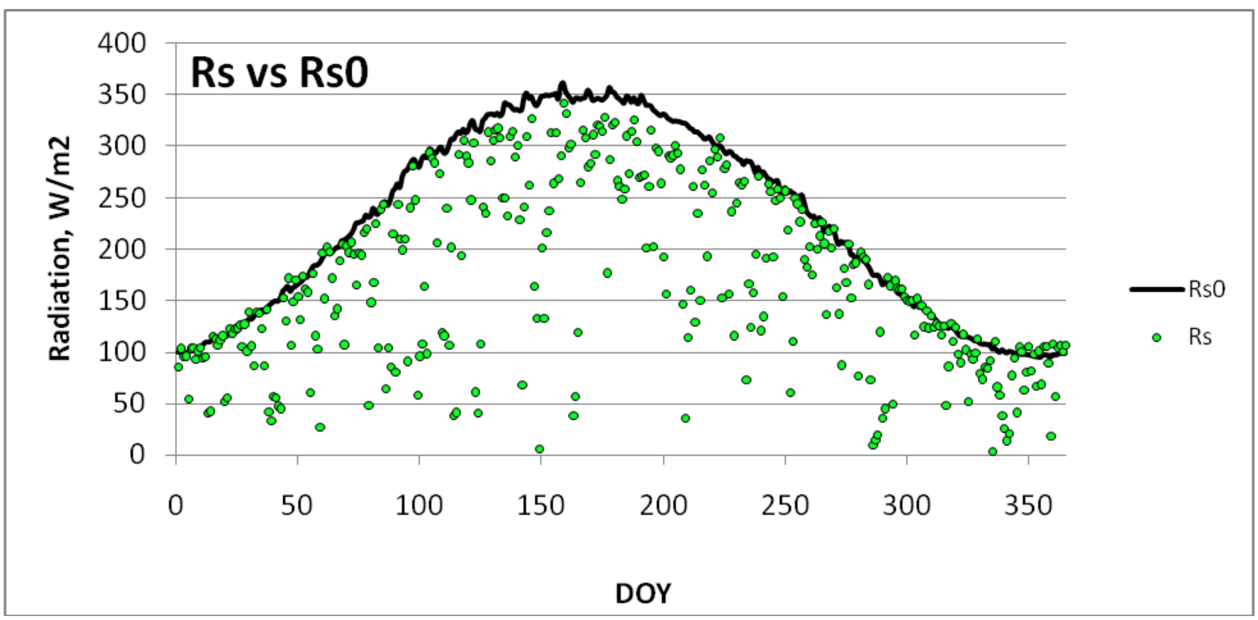

Figure 5. Observed solar radiation (W/m^2) and calculated clear sky solar radiation (W/m^2) for 2007 from the Merna HPRCC AWDN weather station.

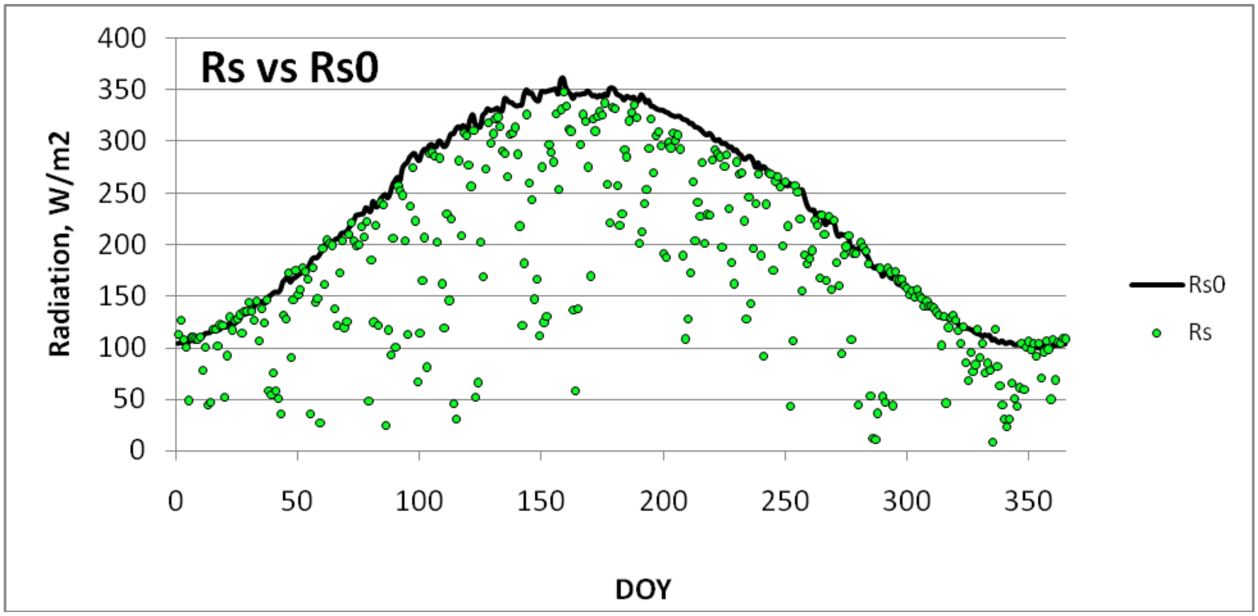

Figure 6. Observed solar radiation (W/m^2) and calculated clear sky solar radiation (W/m^2) for 2007 from the Smithfield HPRCC AWDN weather station.

Daily Soil Water Balance Model

A daily soil water balance model based on Allen et al. (1998) was employed to estimate residual moisture from the bare soil for 2007 for each of the selected weather station for a given Landsat scene. The results from soil water balance were used to determine ET_rF for hot pixel selection, a calibration step for running METRIC model. An example of soil water balance simulations based on soil properties and meteorological data is shown in figure 7 from Central City.

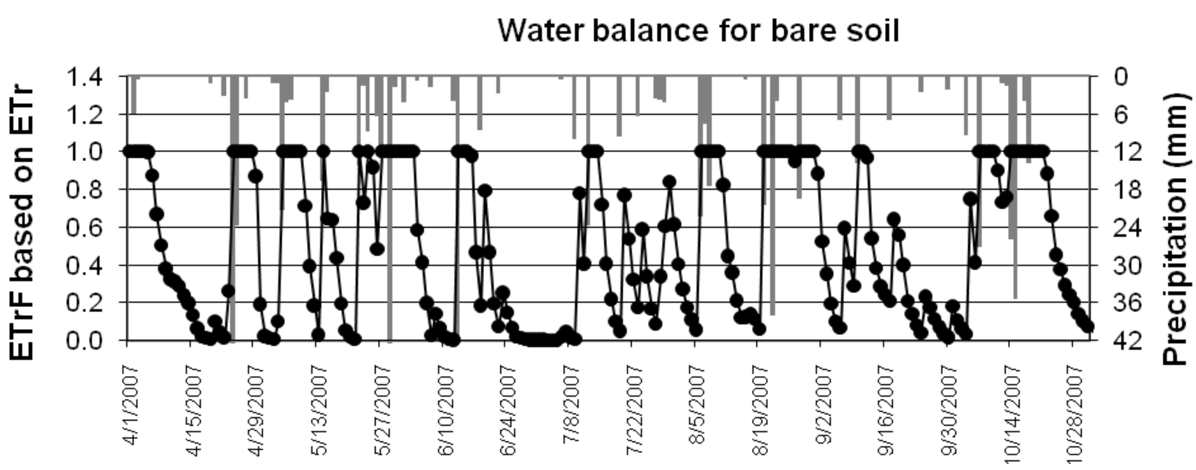

Figure 7. Soil water balance for bare soil calculated from meteorological data from Central City, NE for 2007.

Table 2: Details of satellite images used in this study

Date	Satellite	Sensor	Path	Row
07 April 2007	Landsat 5	TM	29	31
15 April 2007	Landsat 7	ETM^+	29	31
17 May 2007	Landsat 7	ETM^+	29	31
10 June 2007	Landsat 5	TM	29	31
12 July 2007	Landsat 5	TM	29	31
13 August 2007	Landsat 5	TM	29	31
21 August 2007	Landsat 7	ETM^+	29	31
14 September 2007	Landsat 5	TM	29	31
22 September 2007	Landsat 7	ETM^+	29	31
08 October 2007	Landsat 7	ETM^+	29	31
24 October 2007	Landsat 7	ETM^+	29	31
07 April 2007	Landsat 5	TM	29	32
15 April 2007	Landsat 7	ETM^+	29	32
17 May 2007	Landsat 7	ETM^+	29	32
10 June 2007	Landsat 5	TM	29	32
12 July 2007	Landsat 5	TM	29	32
13 August 2007	Landsat 5	TM	29	32
21 August 2007	Landsat 7	ETM^+	29	32
14 September 2007	Landsat 5	TM	29	32
22 September 2007	Landsat 7	ETM^+	29	32
08 October 2007	Landsat 7	ETM^+	29	32
24 October 2007	Landsat 7	ETM^+	29	32
25 November 2007	Landsat 7	ETM^+	29	32
14 April 2007	Landsat 5	TM	30	31
30 April 2007	Landsat 5	TM	30	31
09 June 2007	Landsat 7	ETM^+	30	31
17 June 2007	Landsat 5	TM	30	31
25 June 2007	Landsat 7	ETM^+	30	31
04 August 2007	Landsat 5	TM	30	31
20 August 2007	Landsat 5	TM	30	31
05 September 2007	Landsat 5	TM	30	31
13 September 2007	Landsat 7	ETM^+	30	31
21 September 2007	Landsat 5	TM	30	31
31 October 2007	Landsat 7	ETM^+	30	31
14 April 2007	Landsat 5	TM	30	32
30 April 2007	Landsat 5	TM	30	32
08 May 2007	Landsat 7	ETM^+	30	32
16 May 2007	Landsat 5	TM	30	32
09 June 2007	Landsat 7	ETM^+	30	32
17 June 2007	Landsat 5	TM	30	32
25 June 2007	Landsat 7	ETM^+	30	32
04 August 2007	Landsat 5	TM	30	32
20 August 2007	Landsat 5	TM	30	32
05 September 2007	Landsat 5	TM	30	32
13 September 2007	Landsat 7	ETM^+	30	32
31 October 2007	Landsat 7	ETM^+	30	32

Satellite Imagery

A total of 45 Landsat images from path/row: 29/31, 29/32, 30/31, and 30/32 were acquired from the USGS Earth Explorer data clearinghouse for 2007 (Table 2). Images were acquired as systematic terrain-corrected (Level 1T), 30 meter spatial resolution, with cubic-convolution re-sampling method. The thermal band was re-sampled to 30 meters. The projection and datum used were UTM zone 14 and WGS 1984, respectively. The satellite overpass times were acquired from the image meta data files to estimate zenith angle of the sun, instantaneous values of wind speed at 200 m, air humidity, and ET_r.

Gap-filling of Landsat 7 ETM+ due to the failure of the Scan Line Corrector (SLC)

On May 31, 2003, image data from the ETM+ sensor onboard the Landsat 7 satellite began exhibiting "striping" artifacts (USGS, 2008). It was determined that the problem was a result of the failure of the Scan Line Corrector (SLC) which compensates for the forward motion of the satellite. The post-SLC failure images of Landsat 7 are termed as SLC-off images. Due to the SLC failure, about 22% of the scene area is missing in SLC-off images. Processing of SLC-off images required replacing the missing data. Various approaches are used for filling the missing data. Some of these approaches use data from the previously acquired images to replace the missing pixels. However, this approach is not very useful for agricultural applications due to temporal dynamics. Because Landsat 7 was still able to acquire imagery, the USGS developed new image products to fix the striping problem by combining two separate dates or by interpolation to fill in the data gaps.

We carried out our own correction to the scan line correction for Landsat7 datasets by using convolution filtering (nearest neighborhood method) with a 5X5 pixels majority function (Singh, Irmak et al., 2008). In our application, we have used the approach of gap filling utilizing same time images with spectral information from the neighboring pixels. For this, the convolution filtering algorithm with majority function has been used to replace the missing data. The majority function is preferred due to our overall objective of estimating ET from the agricultural fields. This technique works perfectly for the inner missing lines. However, the missing pixels at the edges of the image scene are not well represented due to large gaps. Hence, it is advisable to subset the images leaving the outer edges.

Preparation of Digital Elevation Model and Land Use Map

The Digital Elevation Model (DEM) used in our processing was obtained from the EROS Data Center Seamless Data Distribution System. The DEM data were then "mosaicked" together in order to provide a single, seamless dataset for each scene to be used in METRIC.

METRIC does not require a land cover map but it improves the parameterization and estimation of the surface roughness parameter (Allen et al., 2007). Three land use maps were adopted to create a single landuse map for the are: 1997, 2001, and 2005. These landuse maps correspond to the years the COHYST land use maps were generated. The land use maps were re-projected into WGS 84, UTM 14 using nearest neighbor re-sampling.

For areas within the Nebraska state boundary, the Nebraska GAP map was used for non-agricultural classes and a COHYST map was used for agricultural classes. The COHYST data extends across the Nebraska border by 2 miles. Due to the different land use systems having the same values for different classes, NE GAP and NE COHYST values were changed. Values for non-agricultural classes in the COHYST data were then reclassified. The land use classes used in this study are listed in appendix A.

Generation of Daily ET Maps with METRIC

Daily ET images were generated from Landsat 5 and Landsat 7 satellite imagery using the METRIC model. Each satellite image for 2007 was processed on a pixel by pixel basis using METRIC to estimate land surface energy balance fluxes. Meteorological data used for the model inputs came from the respective AWDN weather stations.

Some satellite images were acquired immediately after rain events. Rain will “saturate” values in the ET maps. This is due to the water balance model accounting for the wet soil and will reduce the range in ET values between cool, irrigated fields and warm, bare soil.

ET cannot be directly estimated for cloud covered land surfaces. Even thin cirrus clouds can lower the values in the satellite thermal band and cause errors in the calculation of sensible heat fluxes. Therefore, it is essential that all satellite imagery be checked for cloud cover and shadows, and be masked out for further processing.

Masked out areas must be filled in so that further image processing can be uniformly applied to an entire image. Linear interpolation is used to fill in ET values for cloud areas of the imagery. Linear interpolation is used instead of the spline interpolation method because the spline method can become speculative when applied for periods as long as several months. Changes in crop growth and condition, and therefore ET, are uncertain for long periods.

ET is highly variable in space and time due to variability in landuse, climatic conditions, soil properties, and management practices. Spatial variation in soil properties affects surface soil evaporation and surface energy balances, causing within-field and across field variability in ET. Satellite remote sensing provides an opportunity for representing spatial and temporal variation of ET.

Generation of Monthly ET Maps

In order to produce monthly and seasonal ET maps, individual ET_rF maps generated from METRIC were interpolated using a spline model. The spline model is deterministic interpolation method which fits a mathematical function through data points to create a surface (Hartkamp, 1999). The spline surface was achieved through weights (λ_i) and number of points (N). Regularized spline was used because the method results in a smoother surface, but interpolated values may lie outside the known data range. The weight parameter defines the weight of the third derivatives of the surface in the curvature minimization. Higher weight creates a smoother gridded surface. We used following spline function (Franke, 1982):

$$S(x,y) = T(x,y) + \sum_{j=1}^{N} \lambda_j R(r_j) \qquad (1)$$

where T is the constant trend and where r_j is distance from the point (x, y) to the j^{th} point, R is a weighted function of the distance between interpolated point and j^{th} data point (j =1, 2, 3,., N). N is the number of known points. For the regularized spline, T and R are defined as following:

$$T(x,y) = a_1 + a_2x + a_3y \qquad (2)$$

$$R(r) = \frac{1}{2\pi}\left\{\frac{r^2}{4}\left[\ln\left(\frac{r}{2\pi}\right) + c - 1\right] + \tau^2(K_o\left(\frac{r}{\tau}\right) + c + \ln\left(\frac{r}{2\pi}\right))\right\} \qquad (3)$$

where τ^2 is the parameters entered at the command line, r is distance between the point and the sample, K_o is modified Bessel function, and c is constant (0.577215). Coefficients a_1, a_2, and a_3 in Eqn. (5) are found by the solution of a system of linear equations.

Using spline interpolation of daily ET maps, monthly ET maps were generated falling under footprint of Landsat image of path 29 row 31 for the months of May, June, July , August, and September (Figure 8-12) .

The main crops grown in the area are corn and soybean. Corn is usually planted in early May and soybeans are planted in mid May to early June. Both crops are usually harvested in early to mid October. The dominant irrigation method in the area is center pivot and irrigation season is generally from mid June to mid September. The monthly ET maps generated by the METRIC model showed a good progression of ET during the growing season as surface conditions continuously changed (Figure 8-12). The monthly ET was low in the beginning of the season in the upper and the eastern part of in path 29 row 31 (Figure 8). With the progression of the season, monthly ET increased considerably. The cumulative population of monthly ET pixels indicated that the majority of the pixels reached to the highest monthly ET during July (Figure 13). Subsequently, monthly ET decreased and hence the cumulative population curves shifted leftward. It can be also seen that the shape of the cumulative population curve for the month of June is different from the other curves. This is due to cloud cover masking for monthly ET map in June.

Work in Progress. Methodology for cloud filling is underway for all the images having cloud/shadow and background evaporation due to a recent rain event. The distribution of cloud/shadow within the daily ET map has been digitized. The figures presented in this report include results from our efforts that included cloud-filling, but will be replaced with another cloud filling algorithm.

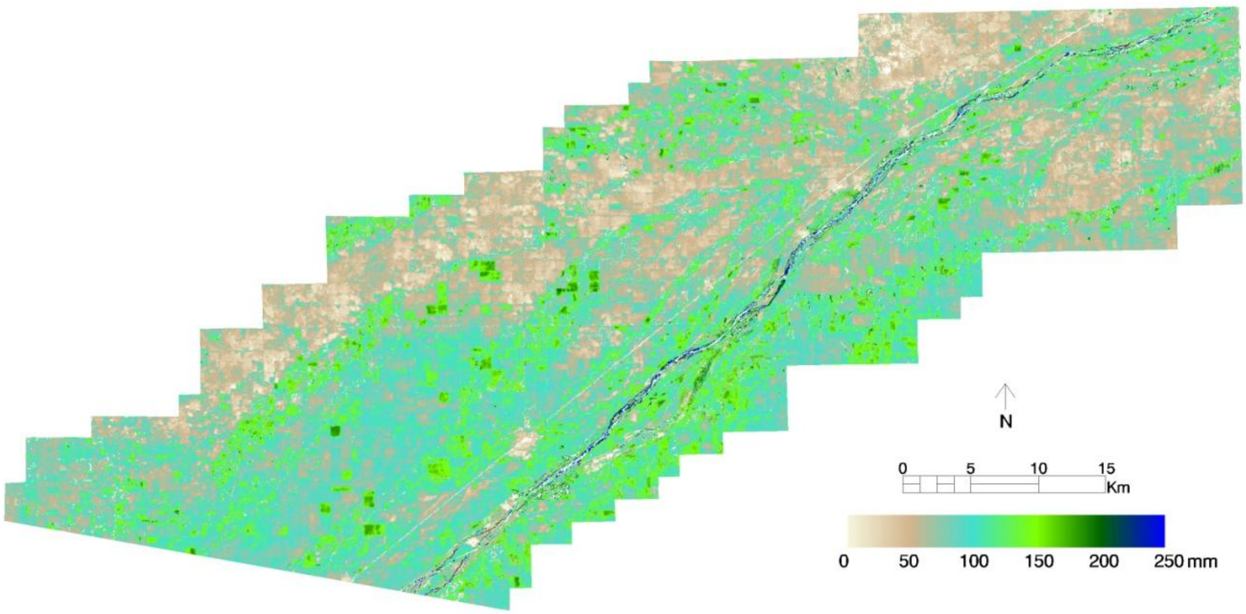

Figure 8. Monthly ET for May 2007 (Path 29 Row 31).

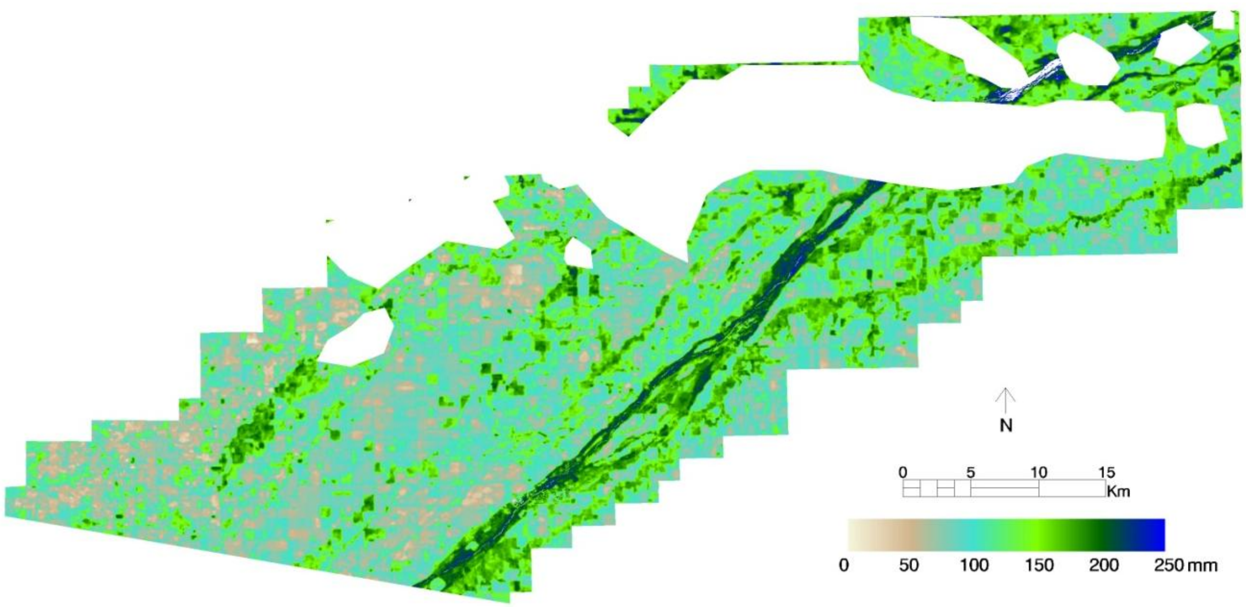

Figure 9. Monthly ET for June 2007 (Path 29 Row 31). White areas are masked out due to clouds.

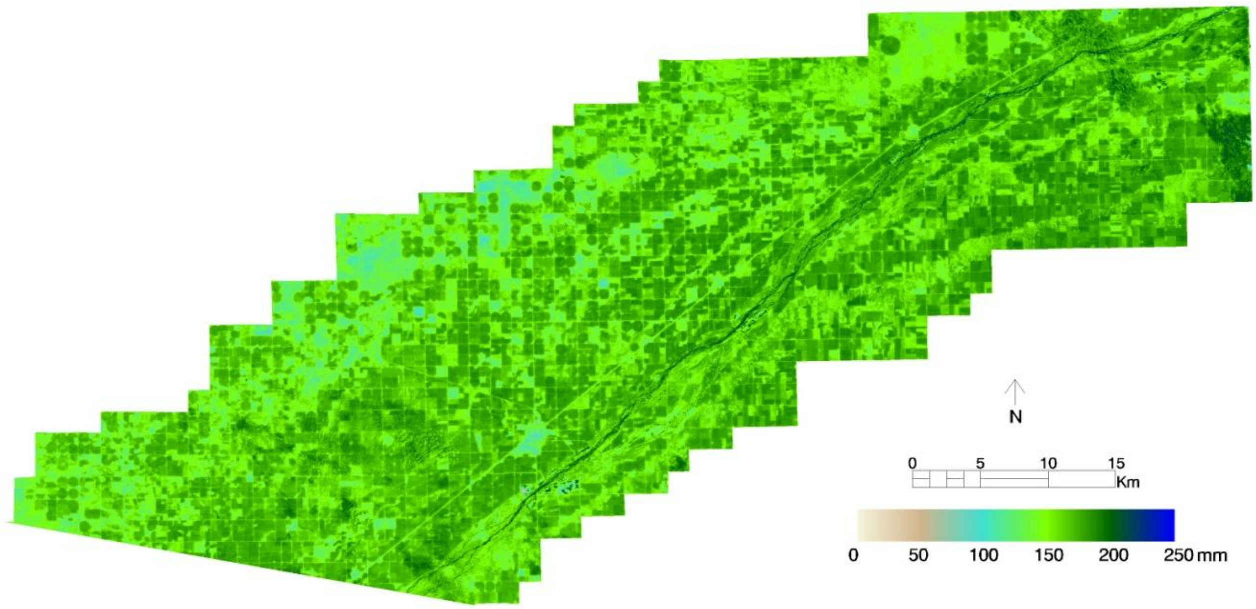

Figure 10. Monthly ET for July 2007 (Path 29 Row 31).

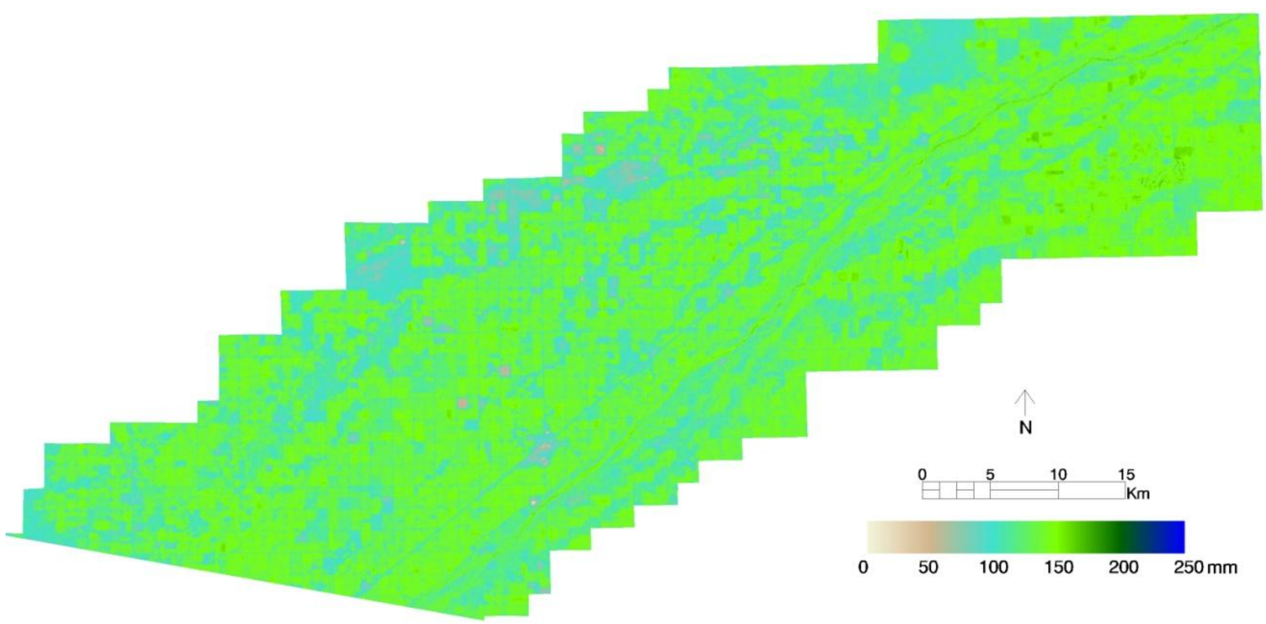

Figure 11. Monthly ET for August 2007 (Path 29 Row 31).

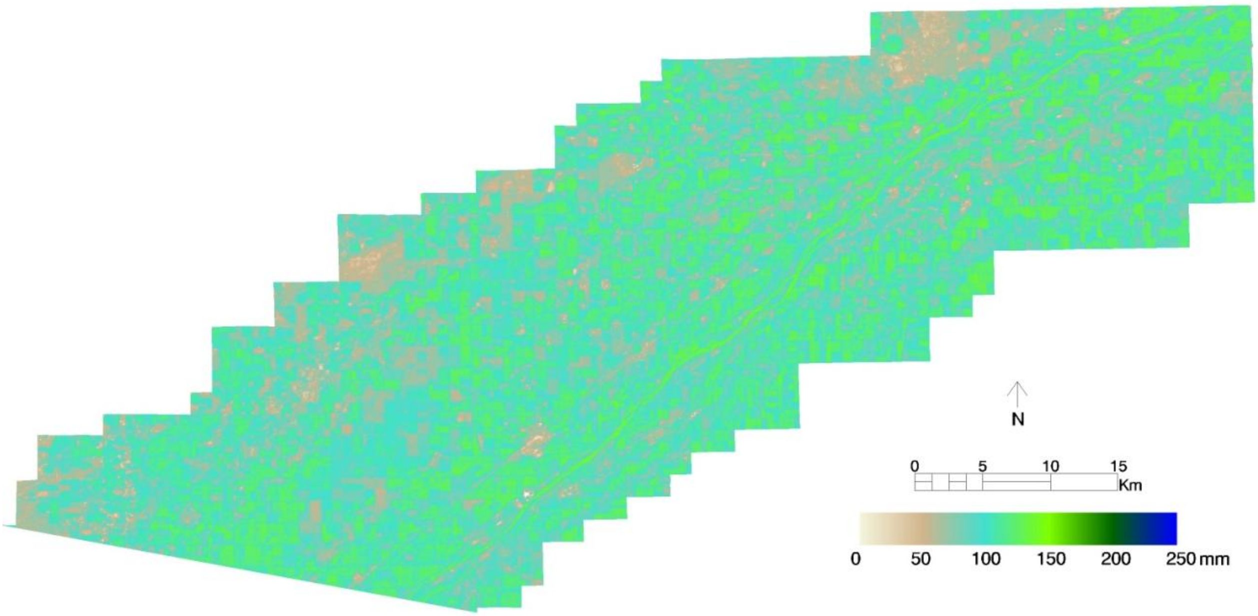

Figure 12. Monthly ET for September 2007 (Path 29 Row 31).

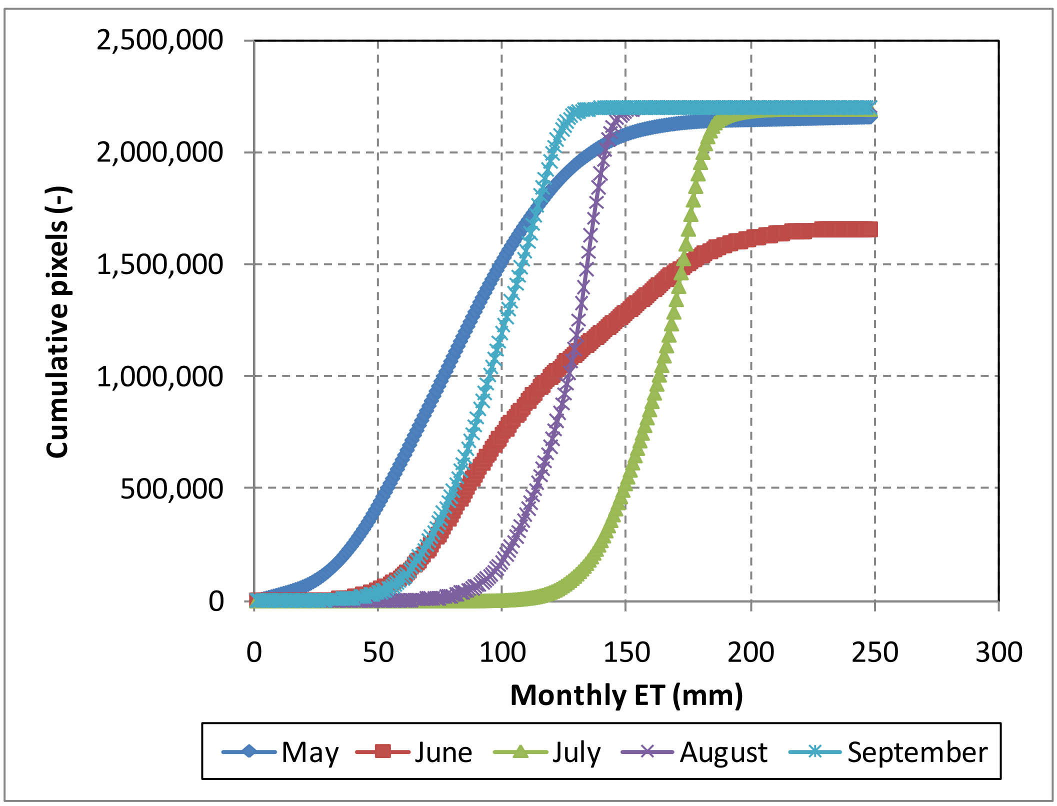

Figure 13. Cumulative population of monthly ET pixels (Path 29 Row 31).

Land use classes used in the calculation of surface roughness in METRIC model.

Class #	Dataset	Category
11	NLCD	Water
21	NLCD	Developed, open space
22	NLCD	Developed, low density
23	NLCD	Developed, medium density
24	NLCD	Developed, high density
31	NLCD	Barren land
41	NLCD	Deciduous forest
42	NLCD	Evergreen forest
52	NLCD	Shrub
71	NLCD	Grassland
81	NLCD	Pasture/hay
82	NLCD	Cultivated crops
90	NLCD	Woody wetlands
95	NLCD	Emergent herbaceous wetland
101	NE-GAP	Ponderosa Pine forests and woodlands
102	NE-GAP	Deciduous Forest/Woodlands
103	NE-GAP	Juniper Woodlands
104	NE-GAP	Sandsage shrub land
105	NE-GAP	Sandhills upland prairie
106	NE-GAP	Lowland tall grass prairie
107	NE-GAP	Upland tall grass prairie
108	NE-GAP	Little Bluestem-Gramma mixed grass prairie
109	NE-GAP	Western Wheatgrass mixed grass prairie
110	NE-GAP	Western short grass prairie
111	NE-GAP	Barren/sand/outcrop
112	NE-GAP	Agricultural fields
113	NE-GAP	Open water
114	NE-GAP	Fallow agricultural fields
115	NE-GAP	Aquatic bed wetland
116	NE-GAP	Emergent wetland
117	NE-GAP	Riparian shrub land
118	NE-GAP	Riparian woodland
119	NE-GAP	Low intensity residential
120	NE-GAP	Commercial/Industrial/Transportation
121	COHYST	Irrigated corn
122	COHYST	Irrigated sugar beets
123	COHYST	Irrigated soybeans
124	COHYST	Irrigated sorghum (Milo, Sudan)
125	COHYST	Irrigated dry edible beans
126	COHYST	Irrigated potatoes
127	COHYST	Irrigated alfalfa
128	COHYST	Irrigated small grains
135	COHYST	Irrigated sunflower
136	COHYST	Summer fallow
138	COHYST	Dryland corn
139	COHYST	Dryland soybeans
140	COHYST	Dryland sorghum
141	COHYST	Dryland dry edible beans
142	COHYST	Dryland alfalfa
143	COHYST	Dryland small grains
144	COHYST	Dryland sunflower